1218 *Macromolecules* **2010**, *43*, 1218–1226
DOI: 10.1021/ma9024043

Macromolecules
ARTICLE

Effect of PAMAM Dendrimers on *$Ru(bpy)_3^{2+}$ Emission Quenching by Ferrocyanide and on ANS Fluorescence: Quantitative Binding Parameters as a Function of Dendrimer Size, pH, and Buffer Composition

Tony Frost and Lawrence D. Margerum*

Department of Chemistry, University of San Francisco, San Francisco, California 94117

Received October 29, 2009; Revised Manuscript Received December 17, 2009

ABSTRACT: The quenched emission intensity for *$Ru(bpy)_3^{2+}$ in the presence of ferrocyanide, [$Fe(CN)_6^{4-}$], was restored in aqueous solutions at pH 8 via the addition of PAMAM dendrimers due to competitive electrostatic binding of the ferrocyanide to the dendrimer. Binding equations were developed assuming a 1:1 interaction between the quencher and a dendrimer binding site size (defined as the number of terminal amine groups). Nonlinear curve fitting of titration data for emission intensity versus added dendrimer at fixed [$Fe(CN)_6^{4-}$] resulted in calculated values for the binding constants, binding site sizes, and bound quenching rate constants between ferrocyanide and different sized dendrimers. When the PAMAM dendrimer size was increased, the ferrocyanide binding constant increased and the fully bound quenching rate constant decreased, but the binding site size remained the same (between 5 and 6 terminal amines). Changing the buffer from Tris to phosphate at pH 8 dramatically changes the binding parameters as predicted for primarily electrostatic binding. Direct binding studies using solvatochromic 8-anilino-1-naphthalenesulfonic acid (ANS) emission and PAMAM dendrimers indicated a large hydrophobic change going from G3 to G4 that was not seen for ferrocyanide binding. ANS binding constants increased going from pH 6 to 8, which may be explained by the unique protonation behavior and macromolecular topology of PAMAM dendrimers.

Introduction

Dendrimers are a novel class of hyperbranched macromolecules that consist of a polyfunctional core with shells of monomer units extending off of branching points.[1,2] The resulting macromolecules have well-defined molecular weights, sizes, and end-group functionalities. An explosion of unique applications has recently appeared in the dendrimer literature in such areas as macromolecular catalysis,[3−6] drug delivery,[7−11] MRI contrast agents,[12−15] surface modifications,[16−20] and metal ion binding.[21−25] The appeal of dendrimeric macromolecules is the ability to tailor the structure, shape, and surface functional groups for the application desired.

Perhaps the best-known and studied water-soluble dendrimers are the poly(amidoamine) or PAMAM series of Starburst dendrimers, which are referred to by their generation number, G*X*.0 (where *X* is 0, 1, 2, ..., *X*.0 is a full generation terminating in primary amines, and *X*.5 is a half-generation terminating in carboxylic acids).[26] Potentiometric titrations and computer simulations on PAMAM dendrimers showed some unique protonation behavior compared to other amine-based dendrimers. Borkovec and co-workers used a site binding model to conclude that the outer primary amines on large PAMAM dendrimers protonate at high pH (microstate pK = 9.0) while the interior tertiary amines only protonate at low pH.[27] Crooks and co-workers came to a similar conclusion and included ionic strength factors that showed the outer amines were more sensitive to ionic strength effects than interior amines with pK_a increasing from 9.15 at I = 29 mM to 9.30 at I = 129 mM. Relevant to this work, they concluded that negative counterions easily penetrated PAMAM dendrimers and that at pH 8 no interior amines were charged, while approximately 80−90% of the outer amines were charged.[28]

Photochemical and optical absorption differences caused by the addition of small molecule probes to PAMAM dendrimers supported a structural change in which the open fluxional lower generations of G2.5 or less transformed to a more rigid spherical structure by G3.5 and beyond.[29,30] Conversely, there was some disagreement as to the effect of solvent and pH on the size and location of terminal groups for the PAMAM series.[31,32] These are important points to resolve as a number of potential applications for dendrimers, including drug delivery and metal ion extraction, require an understanding of small molecule binding as a function of changes in the aqueous environment.

This study extends our previous electrochemical binding method in which diffusion currents decrease for highly charged inorganic complexes that bind to PAMAM dendrimers.[33] The technique employed for the work described in this report comes from Thorp et al. in their study of metal complexes that bind with DNA. They used the anionic chromophore $Pt_2(pop)_4^{4-}$ (pop = $P_2O_5H_2^{2-}$), which was repelled by the polyanionic sugar−phosphate backbone of the DNA, and measured the quenching rate constant with complexes such as $Co(phen)_3^{3+}$ in the presence and absence of DNA. They found the quenching rate constant between *$Pt_2(pop)_4^{4-}$ and $Co(phen)_3^{3+}$ decreased dramatically in the presence of DNA due to ionic binding.[34] Turro and Tomalia have done extensive work on chromophore−PAMAM dendrimer binding, such as for *$Ru(phen)_3^{2+}$ quenching by $Co(phen)_3^{2+}$.[35] They found that the *$Ru(phen)_3^{2+}$ emission was enhanced when bound by the carboxylic acid-terminated dendrimers (G4.5 to G8.5) due to decreased quenching by oxygen. They inferred that the dendrimer surface had a lower

*Corresponding author. E-mail: margeruml@usfca.edu.

 Published on Web 01/14/2010

Table 1. Select Properties and Calculated Molar Concentrations of Commercially Available PAMAM Dendrimer Solutions in MeOH (ED Core)

generation (*x*.0)	terminal amines (*n*)	molar mass (g mol^{-1})	wt % nominal	density (g mL^{-1})	[$G_{x.0}$] (mM)[a]
0.0	4	516.68	20	0.854	330.6
1.0	8	1429.85	20	0.82	114.7
2.0	16	3256.19	20	0.86	52.8
3.0	32	6908.87	20	0.863	25.0
4.0	64	14214.23	10	0.813	5.7
5.0	128	28824.95	10	0.797	2.8

[a] The certificate of analysis was used for the actual concentrations.

oxygen concentration than water and derived a PAMAM half-generation to $Ru(phen)_3^{2+}$ binding constant of $5.0 \times 10^5\ M^{-1}$. In general, relatively few studies exist that systematically probe the effects of dendrimer microenvironment, or their end groups, on small molecule binding behavior in aqueous buffered solutions.

In this study we describe a method to elicit binding information between a charged small molecule probe and PAMAM dendrimers in buffered aqueous solutions. The technique is to measure the emission intensity of $*Ru(bpy)_3^{2+}$ in the presence of the quencher ferrocyanide, $Fe(CN)_6^{4-}$, and monitor the emission intensity while adding amine-terminated PAMAM dendrimers. The observed increase in emission intensity occurs due to electrostatic binding of ferrocyanide to the protonated amines sites on the slower diffusing dendrimer. The data are modeled by equations adapted from the literature on metal complexes that bind to DNA in order to obtain microscopic binding constants, quenching rate constants, and binding site sizes to PAMAM dendrimers for the first time. The technique is fast, uses minimal amounts of materials, and potentially gives valuable insight into the microenvironments of a wide variety of water-soluble dendrimers.

Materials and Methods

Materials. Methanolic solutions of Starburst polyamidoamine (PAMAM) dendrimers with an ethylenediamine (ED) core were purchased from Sigma-Aldrich. The certificate of analysis was used to calculate the true stock solution concentration using the wt %, the density, and the calculated molar mass (Table 1).

Other materials used were of research quality. Potassium ferrocyanide trihydrate, $K_4[Fe(CN)_6]\cdot 3H_2O$, was from EM Sciences (Cherry Hill, NJ), sodium chloride and phosphate buffer salts were from J.T. Baker (Phillipsburg, NJ), tris(hydroxymethyl)aminomethane (Tris), $H_2NC(CH_2OH)_3$, and 8-anilino-1-naphthalenesulfonic acid (ANS) were from Sigma-Aldrich, and tris(bipyridine)ruthenous chloride hexahydrate, $[Ru(bpy)_3]Cl_2\cdot 6H_2O$, was from GFS Chemicals (Columbus, OH).

Methods. A SPEX FluoroMax-P (Horiba Jobin Yvon) with FluorEssence software was used for all measurements and was calibrated with triple distilled water. Cuvettes were cleaned with detergent, soaked overnight in 8 M nitric acid, and thoroughly washed with deionized water before each use. A circulating water bath maintained the cuvette at 23.0 °C.

All solutions were prepared using distilled water from a Corning Mega-Pure purification system. The acidic and basic forms of buffers were mixed, with added NaCl, to achieve 5 mM buffer and 50 mM NaCl before adjusting the desired pH with HCl. A 100 μM ferrocyanide stock solution was made by mixing the correct mass with a buffered 8 μM $Ru(bpy)_3^{2+}$ stock solution in volumetric glassware so as to minimize dilution effects during titrations. The desired amount of methanolic dendrimer solution was transferred to a tube via digital pipet and the methanol removed via evaporation. Exactly 3.0 mL of the ferrocyanide/$Ru(bpy)_3^{2+}$ solution was delivered to the test tube and mixed. The ANS/dendrimer solutions were prepared in a similar fashion except that the ANS was first dissolved in 0.5 mL of *N,N*-dimethylformamide (DMF), and then buffered saline solution was added to make a 20 μM solution.

For titrations, aliquots (20 μL) of the stock dendrimer solution were added via calibrated digital pipet to a volume of the target solution in the cuvette. An emission spectrum was obtained following each addition. The maximum emission intensity, I_x, was recorded at the peak wavelength. The excitation wavelength, λ_{ex}, was 452 nm for $Ru(bpy)_3^{2+}$ and was 370 nm for ANS. All emission spectra were recorded between 480 and 800 nm.

Prism 4.0 curve fitting software from GraphPad was used to fit data sets to the binding isotherm equation using nonlinear regression. Normally two data sets were fit simultaneously (global fitting), giving excellent fits to the model and one shared value for each variable.

Derivation of the Binding Model. The equilibrium binding equation and equilibrium expression between a probe molecule (P) and a binding site (S) are

$$P + S \rightleftharpoons PS \quad K = \frac{[PS]}{[P][S]} \quad \text{or} \quad [PS] = K[P][S] \tag{1}$$

where [PS] is the measured concentration of bound species and [P] and [S] are the concentrations of free probe and free binding sites, respectively. The total molar concentration of a full dendrimer generation, *x*.0, is defined by [G_x]. Thorp and coworkers adapted a neighbor-exclusion binding model, first used by Bard,[36] to determine large binding constants to DNA via emission quenching of $Pt_2(pop)_4^{4-}$. In the model, *s* is the size of the binding site in DNA base pairs. As dendrimers do not have base pairs, we choose to define the size of the binding site in terminal amines, *s*. Given that a dendrimer has a total of *n* terminal amines (Table 1), and assuming each binding site has the same number of terminal amines, leads to the total number of possible binding sites on a dendrimer, $S = n/s$. The total *concentration* of binding sites, $[S]_t$, is then defined in eq 2, which may be rearranged into eq 3.

$$[S]_t = \frac{n}{s}[G_x] = [S] + [PS] \tag{2}$$

$$[S] = \frac{n}{s}[G_x] - [PS] \tag{3}$$

Likewise, the total probe concentration is $[P]_t = [P] + [PS]$, leading to $[P] = [P]_t - [PS]$. Appropriate substitutions into eq 1 followed by isolation of the term for the product gives

$$[PS] = \frac{K[P]_t[S]}{1 + K[S]} \tag{4}$$

Similarly, substituting (3) into (4) leads to an equation relating the bound species concentration to the total probe concentration and the total dendrimer concentration, both known in the experimental setup.

$$[PS] = \frac{K[P]_t\left(\frac{n}{s}[G_x] - [PS]\right)}{1 + K\left(\frac{n}{s}[G_x] - [PS]\right)} \tag{5}$$

Equation 5, rearranged into a quadratic equation, gives eq 6, where the variable is [PS].

$$K[\mathrm{PS}]^2 - \left(K\frac{n}{s}[\mathrm{G}_x] + K[\mathrm{P}]_t + 1\right)[\mathrm{PS}] + K\frac{n}{s}[\mathrm{G}_x][\mathrm{P}]_t = 0 \quad (6)$$

Solving for [PS] from the quadratic formula yields eq 7

$$[\mathrm{PS}] = \frac{1 + K[\mathrm{P}]_t + K\frac{n}{s}[\mathrm{G}_x] - \left(\left(1 + K[\mathrm{P}]_t + K\frac{n}{s}[\mathrm{G}_x]\right)^2 - 4K^2\frac{n}{s}[\mathrm{G}_x][\mathrm{P}]_t\right)^{1/2}}{2K} \quad (7)$$

We need to know X_b, the fraction of bound probe, at various concentrations of dendrimer in order to derive the binding isotherm. The term X_b needs to be measured at each dendrimer concentration using a signal whose strength is dependent on dendrimer concentration. The quenching rate constant between ferrocyanide and the ruthenium complex is such a signal. The free and fully bound quenching rate constants of this couple are given by k_{q_f} and k_{q_b}, respectively. The term k_{q_x} defines the observed quenching rate constant at a given concentration of dendrimer. Equation 8 defines the fraction of bound probe, X_b, in terms of quenching rate constants, k_q.

$$X_b = \frac{k_{q_x} - k_{q_f}}{k_{q_b} - k_{q_f}} = \frac{[\mathrm{PS}]}{[\mathrm{P}]_t} \quad (8)$$

In addition, the Stern−Volmer relationship can be utilized (9) for it defines how probe-quencher concentration, $[P]_t$, affects the emission intensity, I, compared to the intensity in the absence of quencher, I_0 (the emission lifetime is τ).

$$\frac{I_0}{I} = 1 + k_q\tau[P]_t \quad (9)$$

and

$$k_{q_x} = \frac{\frac{I_0}{I} - 1}{\tau[\mathrm{P}]_t} \quad (10)$$

In order to obtain an expression for the fraction of bound probe, X_b, we divide eq 7 by $[P]_t$.

$$\frac{[\mathrm{PS}]}{[\mathrm{P}]_t} = \frac{1 + K[\mathrm{P}]_t + K\frac{n}{s}[\mathrm{G}_x] - \left(\left(1 + K[\mathrm{P}]_t + K\frac{n}{s}[\mathrm{G}_x]\right)^2 - 4K^2\frac{n}{s}[\mathrm{G}_x][\mathrm{P}]_t\right)^{1/2}}{2K[\mathrm{P}]_t} \quad (11)$$

Combining eqs 8, 10, and 11 gives the operative binding model in eq 12, which relates the change in emission intensity for fixed values of [P] as a function of $[G_x]$ using the variables K, s, k_{q_f}, and k_{q_b}.

$$\frac{I_0}{I} - 1 = \left(\left(\frac{1 + K[\mathrm{P}]_t + K\frac{n}{s}[\mathrm{G}_x] - \left(\left(1 + K[\mathrm{P}]_t + K\frac{n}{s}[\mathrm{G}_x]\right)^2 - 4K^2\frac{n}{s}[\mathrm{G}_x][\mathrm{P}]_t\right)^{1/2}}{2K[\mathrm{P}]_t}\right)(k_{q_b} - k_{q_f}) + k_{q_f}\right)\tau[\mathrm{P}]_t \quad (12)$$

Our binding model assumes that the charged quencher P, ferrocyanide, binds to discrete binding sites, S, of size s number of primary amines on the dendrimer. This assumption does not require that the primary amines be located perfectly at the periphery of an imaginary sphere. In fact, computational evidence suggests that this is almost never the case for dendrimers.[37,38] The binding site size s must be less than or equal to the number of primary amines n of the generation being investigated. We also assume that the majority of the observed binding interactions are electrostatic between protonated primary amines and the tetra-anionic ferrocyanide.

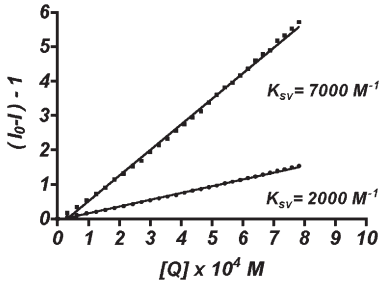

Figure 1. Stern−Volmer plots for the quenching of 8 μM *$Ru(bpy)_3^{2+}$ by $Fe(CN)_6^{4-}$ in pH 8 Tris buffer. Upper line has no added salt and lower line has 50 mM NaCl. λ_{ex} = 452 nm and λ_{em} = 610 nm.

Results and Discussion

Collision of a quencher molecule, Q, with a fluorophore in a long-lived excited state may deactivate the excited state by means of energy transfer or electron transfer (oxidation or reduction). In either case the emission intensity, I_0, is reduced to I by an amount proportional to the quencher concentration, [Q], which is described by the Stern−Volmer relationship[39]

$$\frac{I_0}{I} = 1 + k_q\tau_0[\mathrm{Q}] = 1 + K_{SV}[\mathrm{Q}] \quad (13)$$

where k_q is the bimolecular quenching constant, τ_0 is the lifetime of the chromophore in the absence of quencher, and the quenching constant, K_{SV}, is defined as $k_q\tau_0$. A plot of $(I_0/I) - 1$ versus [Q] should go through the origin and have a slope K_{SV}. Ferrocyanide is a reductive quencher to *$Ru(bpy)_3^{2+}$ in water, producing transient amounts of $Fe(CN)_6^{3-}$ and $Ru(bpy)_3^{1+}$ with a quenching rate constant, k_q, of 3.3×10^9 M^{-1} s^{-1} (τ_0 = 360 μs) in aerated 0.5 M NaCl at 20 °C.[40−42] Figure 1 is a Stern−Volmer plot for the quenching of *$Ru(bpy)_3^{2+}$ by $Fe(CN)_6^{4-}$ under the buffer and salt conditions of this study.

Using the slope and assuming the lifetime of the excited state is 360 μs,[41] we obtain $k_q = 19 \times 10^9$ M^{-1} s^{-1} in the presence of 5 mM Tris at pH 8 and 5.6×10^9 M^{-1} s^{-1} with added 50 mM NaCl in this buffer. These values are consistent with electrostatic, diffusional quenching and can be compared with the calculated k_q from the proposed binding model.

Effect of Added G3.0 on Quenching of *$Ru(bpy)_3^{2+}$ by $Fe(CN)_6^{4-}$. The lowest intensity peak in Figure 2 is the emission spectrum for 8 μM $Ru(bpy)_3^{2+}$ with 100 μM $Fe(CN)_6^{4-}$ dissolved in 5 mM Tris (pH 8.0, 50 mM NaCl). As aliquots of G3.0 PAMAM, a molecule with n = 32 terminal amine arms and a molar mass of over 3200 g/mol, are added into the solution, the intensity *increases* and approaches the emission spectrum for unquenched *$Ru(bpy)_3^{2+}$ (upper most curve).

An examination of Figure 2 shows that the cationic *$Ru(bpy)_3^{2+}$ does not interact with the polycationic dendrimer at pH 8 as the emission peak does not shift throughout the titration. Previous work with the anionic fluorescent probe $Ru(4,7\text{-}(SO_3C_6H_4)_2\text{-phen})_3^{4-}$ showed a shift in its emission maximum as this probe interacted with PAMAM dendrimers.[43] This was not the case for the interaction between

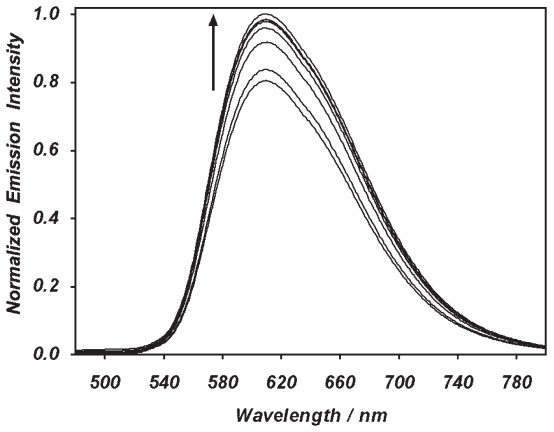

Figure 2. Normalized emission spectra of 8 μM $Ru(bpy)_3^{2+}$. Lowest intensity spectrum is with 100 μM $Fe(CN)_6^{4-}$. Subsequent spectra are after addition of G3.0 (4, 17, 29, 54, 93, and 134 μM bottom to top). [Tris] = 5 mM, [NaCl] = 50 mM, pH 8.0, λ_{ex} = 452 nm, 23 °C in air.

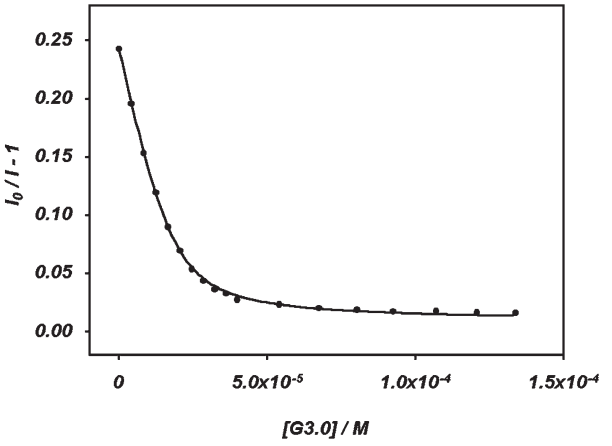

Figure 3. Plot of $I_0/I - 1$ versus [G3.0] for $Ru(bpy)_3^{2+}$ with 100 μM ferrocyanide at pH 8 (Tris) and the nonlinear regression least-squares fit of the data to eq 12.

$Ru(bpy)_3^{2+}$ and anionic half-generation PAMAM dendrimers.[29] Here, adding a large excess of G3.0 (280 μM) to 8 μM $*Ru(bpy)_3^{2+}$ barely changes the signal intensity (−2%). Second, the quenching data show increases in emission intensity as the concentration of G3.0 increases due to the reduced quenching efficiency of the dendrimer bound ferrocyanide compared with free ferrocyanide. Therefore, the electrostatic binding of ferrocyanide to the dendrimer competes with the diffusional quenching of $*Ru(bpy)_3^{2+}$, and the change in signal intensity must be related to a microscopic binding constant between quencher and dendrimer.

Figure 3 is the data from Figure 2 plotted as ($I_0/I - 1$) versus [G3.0], with a nonlinear regression line generated from the binding eq 12 as described in the Materials and Method section. The constants in the titration are $[P]_t$ (100 μM ferrocyanide), n (32 for G3.0), and τ, the emission lifetime of $*Ru(bpy)_3^{2+}$. The measured values are emission intensity, I_0 in the absence and I in the presence of dendrimer concentrations, $[G_x]$. The unknown fitting parameters K, s, k_{q_f}, and k_{q_b} are the microscopic equilibrium binding constant, binding site size in primary amines, and free and bound quenching rate constants, respectively. Individual data sets fit to the binding isotherm model give slightly different values for K and s. To overcome this problem, two data sets are fit simultaneously, which give the highest correlation coefficient and one shared value of K and s, respectively. Adding a third data set does not change the values. Therefore, all plots and the resulting variables for the binding isotherm are global fits using two different data sets.

By measuring the increase in emission intensity with added dendrimer, we are effectively making single point measurements of k_q as the function $I_0/I - 1$ approaches zero. Thus, the first data point (no dendrimer) in Figure 3 is a single point measurement of k_{q_f}. The fit in Figure 3 yields k_{q_f} as 6.8×10^9 M^{-1} s^{-1} compared to 6.5×10^9 M^{-1} s^{-1} for the single data point at [G3.0] = 0. These values are about 20% higher than the value calculated from the Stern−Volmer slope in Figure 1. Thorp and workers noted that the amount of quenching of an excited state was dependent upon the quencher concentration; therefore, they calculated an effective quenching rate constant from the nonlinear binding equation instead of using the Stern−Volmer measurement.[34] As we did not test the effect of ferrocyanide concentration on $*Ru(bpy)_3^{2+}$ emission quenching in the presence of dendrimers, the quenching rate constants here are all calculated from eq 12.

The fully bound quenching rate constant, k_{q_b}, is the residual quenching rate when the dendrimer concentration tends toward infinity in the presence of ferrocyanide (not experimentally accessible). In the case of G3.0 at pH 8.0, the global fit gives k_{q_b} as 2.4×10^8 M^{-1} s^{-1}, which is over 25 times less than the free quenching rate constant, consistent with slower diffusional quenching due to dendrimer−ferrocyanide binding. Therefore, the bound quenching rate must be a function of dendrimer size.

Finally, the best nonlinear regression fit to the data in Figure 3 reveals a microscopic equilibrium binding constant, K, for ferrocyanide binding to the binding sites on G3.0 of 7.3×10^4 M^{-1} and a binding site size, s, of 5.6 terminal amines. While the interpretation of the latter parameter will be discussed below, one must keep in mind that by our definition s includes all terminal amines, not just the charged ones at the pH of interest. While not ideal, we work at pH 8 to make sure *most* terminal amines on a given dendrimer are charged (80−90% based on calculated pK_a ranges in refs 27 and 28), while none of the internal amines carry any charge. Our initial efforts are to control the pH and see the effect of dendrimer size on several binding parameters with the assumption that the protonation state of the terminal amines on PAMAM dendrimers are fairly constant with size. One might expect the binding site size, s, to be equal to four in order to match the charge of ferrocyanide. Yet, the physical meaning of the binding site size parameter is not clear in the literature. For example, cationic metal complexes binding to DNA gave binding site sizes between 3.2 and 4.6 base pairs for Fe(II), Co(III), Os(II), and Ru(II) complexes containing the phen or bpy ligand under a variety of conditions.[34,44] Yet, an s value of 1.6 base pairs was reported for DNA binding with $Ru(NH_3)_6^{3+}$ using steady-state voltammetry at microelectrodes.[45] In this work, we plan on discussing *relative* changes in the binding site size, s, with various dendrimers as there is not enough data to support a trend with different metal complexes or to speculate on the microscopic physical meaning of binding site size.

Effect of Dendrimer Size on Binding Parameters. It is instructive to examine a range of dendrimer generations with the quenching experiment. Our initial hypothesis that steric crowding due to the close packing structure of larger dendrimers[26] might lead to larger binding constants, and perhaps decreased binding site size, is not consistent with the data. First, quenching experiments on PAMAM G0.0 dendrimer for which there are only four terminal amine arms (the pK_a's are 9.56, 9.23, 8.58, and 8.21 for the terminal

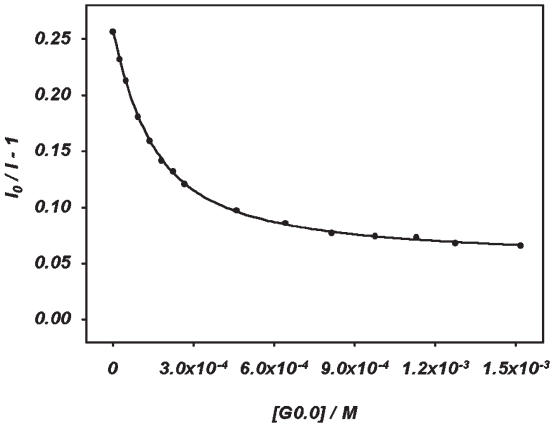

Figure 4. Plot of $I_0/I - 1$ versus G0.0 concentration for $*Ru(bpy)_3^{2+}$ and 100 μM $Fe(CN)_6^{4-}$ at pH 8.0 (Tris + 50 mM NaCl). Nonlinear least-squares fit of data to eq 12.

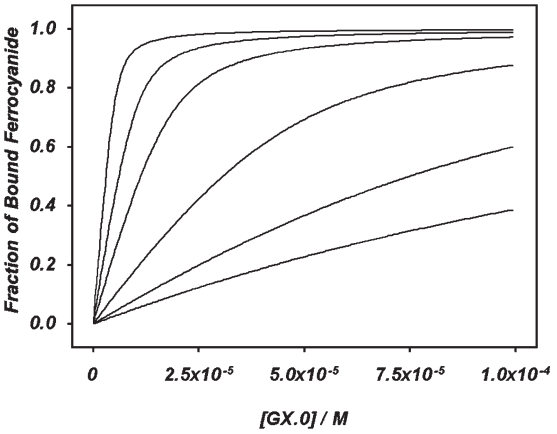

Figure 5. Overlay of the binding isotherms obtained for ferrocyanide and G0.0 to G5.0 (bottom to top) in the presence of 8 μM $Ru(bpy)_3^{2+}$, 100 μM ferrocyanide, 5 mM Tris (pH 8) and 50 mM NaCl. Displayed as the fraction of bound ferrocyanide, X_b, versus dendrimer concentration.

amines and 6.91 and 3.30 for the core tertiary amines)[46] lead to the data in Figure 4. This binding isotherm clearly implies a smaller binding constant than for G3.0 and is confirmed by the fit value of $K = 6.9 \times 10^3$ M^{-1}, which is over an order of magnitude lower than for G3.0. In addition, we note that the binding site size $s = 3.0$ is lower than the limiting number of four charged terminal amines at pH 8.

Based on the pK_a values, at pH 8 there are between three and four charged primary amines on average for this dendrimer. Therefore, a 1:1 electrostatic molecular binding ratio between a G0.0 and one ferrocyanide seems valid (although this has not been validated). Finally, k_{qb} is 1.4×10^9 M^{-1} s^{-1}, indicating that substantial quenching of $*Ru(bpy)_3^{2+}$ still occurs when ferrocyanide is bound to G0.0. This bound quenching rate constant is about 6 times larger than with G3.0. One way to think of this result is to imagine the G0.0 bound ferrocyanide neutralizing almost all of the protonated primary amines on the dendrimer, whereas the G3.0 bound ferrocyanide possesses more (unused) charged terminal amines on average. Therefore, in addition to the faster diffusion rate, the ruthenium cation encounters less electrostatic repulsion with G0.0 than with G3.0.

For ease of understanding, Figure 5 gives all of the binding isotherms (data points not shown) for G0.0 through G5.0 plotted as the fraction of bound ferrocyanide, X_b, versus $[G_x]$. The associated parameters from computer fits to the data are summarized in Table 2.

Table 2. Equilibrium Binding Data between Ferrocyanide and PAMAM Dendrimers in Tris pH 8.0[a]

generation	$K/1 \times 10^3$ M^{-1}	s/binding sites size	$k_{q_f}/1 \times 10^9$ M^{-1} s^{-1}	$k_{q_b}/1 \times 10^9$ M^{-1} s^{-1}
G0.0	6.9	3.0	7.1	1.4
G1.0	24	6.2	7.3	1.0
G2.0	49	6.7	6.9	0.6
G3.0	73	5.6	6.8	0.4
G4.0	94	6.5	6.7	0.1
G5.0	137	6.7	6.9	0.2

[a] Conditions: 8 μM $Ru(bpy)_3^{2+}$, 100 μM $Fe(CN)_6^{4-}$, 5 mM Tris, 50 mM NaCl.

The strength of binding between the probe and dendrimer clearly increases with the fraction of bound probe per given concentration of dendrimer. For example, if a horizontal line were placed at $X_b = 0.5$ (half of all probes bound), G1.0 requires about 0.75 mM dendrimer and G2.0 requires just 0.25 mM. As summarized in Table 2, the binding constants between ferrocyanide and the dendrimer, K, increase almost 20-fold from G0.0 to G5.0. Likewise, k_{q_b} decreases with increasing dendrimer size but may reach a limit, or the measurement is not as sensitive, for G4.0 and G5.0 (note k_{q_f} is constant at 7×10^9 M^{-1} s^{-1}, as expected). A somewhat surprising trend is apparent for the binding site size, s. For G1.0 through G5.0 the number of terminal amines increases (8, 16, 32, 64, and 128, respectively) while the calculated binding site size, s, is relatively constant at five to six primary amines. One way to interpret the binding site size result is that ferrocyanide associates with the space occupied by about six primary amines regardless of dendrimer size. We predicted that the known shape change and denser packing at the PAMAM dendrimer terminal amines past G3.0 (sometimes termed a "static micelle"[47]) might lead to the charge balancing limit of $s = 4$ amines associated with electrostatic binding. This is not the case, although one must be cautious, as the microscopic meaning of the binding site size, s, is not clear. We can only conclude that this parameter is not sensitive to increasing dendrimer size for G1.0 through G5.0. For comparison, the binding site size found for two different DNA intercalators, $Os(phen)_3^{2+}$ and $Co(phen)_3^{3+}$, was 4.0 and 4.6 base pairs, respectively.[44] While a purely electrostatic binding probe may give a closer match of its charge to the binding site size in DNA, this has not been validated.[44] The values of s in excess of the ferrocyanide charge that we see may be due to differences in the nature of DNA and PAMAM dendrimers. DNA has a fixed, regular anionic phosphate backbone while the dendrimer possesses flexible terminal arms with charges governed by the microscopic pK_a's of each amine and the location of those arms (folded in to the interior or exposed on the periphery of the dendrimer). Our results suggest a more extensive exploration is needed of electrostatic binding for different types of dendrimer end groups and sizes. This may give further physical insight into binding site size for small molecule binding to dendrimers.

Effect of Buffer on Binding Parameters. If electrostatic binding of ferrocyanide to PAMAM dendrimer is dominant, then a change in the buffer composition should affect the binding parameters. The pK_a's of phosphoric acid are 2.15, 7.20, and 12.15 at 25 °C.[39,48] Use of the Henderson–Hasselbalch approximation at pH 8 shows that the 5 mM phosphate composition is 0.7 mM $H_2PO_4^-$ and 4.3 mM HPO_4^{2-}. These species will interact electrostatically with the dendrimer and compete with chloride ions from the added NaCl as well as ferrocyanide. The result should be smaller binding constants than for the Tris/TrisH^+ buffer (pK_a 8.08).[39]

The original emission intensity of $*Ru(bpy)_3^{2+}$ does not fully recover in the ferrocyanide−phosphate buffer even at twice the G0.0 concentration compared to Tris (k_{q_f} is unchanged). Therefore, the ferrocyanide to G0.0 binding constant is almost 3-fold smaller ($6.9 \times 10^3 - 2.5 \times 10^3$ M^{-1}). Second, the bound quenching rate constant, k_{q_b}, increases 40% to 2.0×10^9 M^{-1} s^{-1} with phosphate compared to Tris, and the binding site size decreases to 1.7. Thus, there is a strong electrostatic effect for PAMAM dendrimer binding at pH 8 based on differences with these two buffers. All of the microscopic binding constants, K, measured with pH 8 phosphate as a function of dendrimer size are less than those measured in the presence of Tris (Figure 6).

All K values increase with increasing PAMAM generation, but there is a leveling off after G3.0 in phosphate. This leveling off coincides with the known topological shape change from earlier generations (G0.0 to G3.0), which are described as open-dome disklike shapes, to later generations (G4.0 to G5.0), which are described as more spheroid in shape.[49] Ferrocyanide must displace phosphate as the counterion to the protonated primary amine compared to chloride when using Tris. The former is expected to be more difficult and may be reaching a limit by G4.0, or there is an unknown difference in structure with phosphate that causes the leveling off. Clearly, the effect of buffer composition and charge on dendrimer structures and small molecule binding needs clarification.

The bound quenching rate constant is directly related to the ability of the excited state ruthenium chromophore to approach the bound ferrocyanide quencher. This ability would logically decrease as the dendrimer size increases and surface charge density increases. Figure 7 is the change in k_{q_b} values upon increasing the size of the dendrimer in each buffer. As dendrimer size increases, the diffusion rate slows and the electrostatic repulsion toward $Ru(bpy)_3^{2+}$ may increase as the dendrimers accumulate more positive charge.

Again, the data for both buffer systems are consistent as the smallest k_{q_b} values are for the largest sized dendrimers. Interestingly, the bound quenching rate constants in Tris are lower than phosphate for G0.0 to G4.0. Using our assumption, it appears that the anionic phosphates can shield the chromophore from some of the electrostatic repulsion generated on the dendrimer end groups at lower generations, but the effect diminishes by G5.0.

The third important buffer comparison is for the binding site size, s, which is smaller for phosphate than Tris for all generations until G4.0 and G5.0 (Figure 8). Both buffer systems give s values less than four at G0.0 (as expected). The smaller s values in phosphate may be hard to justify based on a physical meaning. Perhaps it represents a competition at the cationic dendrimer binding sites between phosphate and ferrocyanide that is less strong than for chloride in the Tris system. We can say that the more tightly packed spheroid-like higher PAMAM dendrimer generations show little or no difference in the site size parameter at pH 8, which may imply that they present similar surface charge densities or polarities to the charged probe.

Binding of 8-Anilino-1-naphthalenesulfonic Acid (ANS) to PAMAM Dendrimers. To get a more complete picture of the microenvironment of PAMAM dendrimers, we tracked the change in the ANS fluorescence signal during titrations with various sized PAMAM dendrimers. Stryer reported that the quantum yield of ANS in water was almost zero but increased to a value of 0.3 in pure ethanol, while the quantum yield increased and the fluorescence wavelength of ANS decreased as solvent polarity decreased for a series of alcohols.[50] More recently, the ANS anion (Figure 9) showed more than just hydrophobic binding to proteins at low pH as ANS binding by the nonpolar aromatic group and the polar sulfonate group caused shrinkage in the hydrodynamic volume of the proteins.[51] The solvatochromic ANS anion was also used as a probe for the hydrophobic properties of

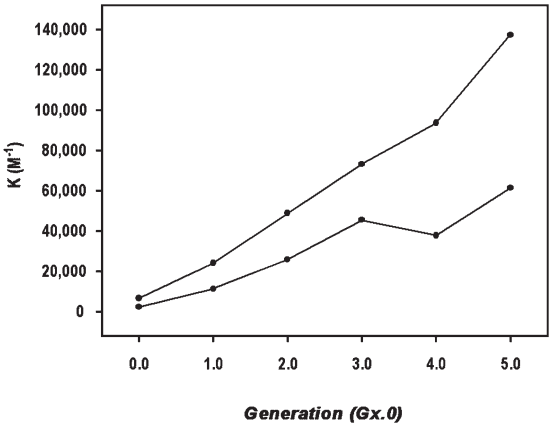

Figure 6. Plot of buffer differences for ferrocyanide and Gx.0 binding constants as a function of dendrimer size. Upper data is 5 mM Tris and lower data is in 5 mM phosphate (both 50 mM NaCl added, pH 8.0). Connecting lines are for visualization only.

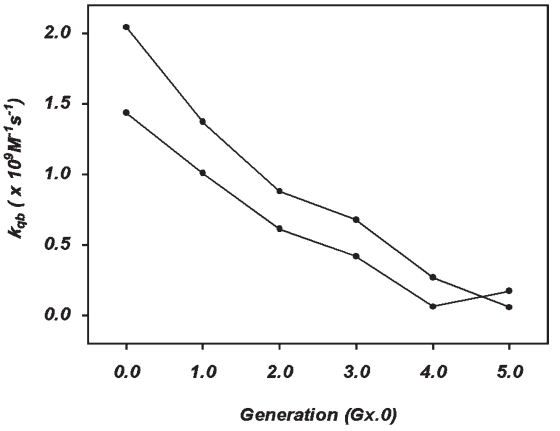

Figure 7. Comparison of the calculated bound quenching rate constant, k_{q_b}, of $*Ru(bpy)_3^{2+}$ by dendrimer bound ferrocyanide (pH 8, 50 mM NaCl). The upper data points are from 5 mM phosphate and the lower data is from 5 mM Tris.

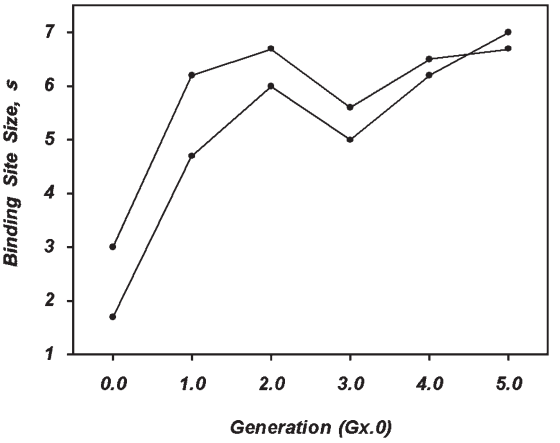

Figure 8. Comparison of calculated binding site sizes, s, for ferrocyanide on dendrimers using pH 8 Tris (upper data line) and pH 8 phosphate (lower data line) (50 mM NaCl).

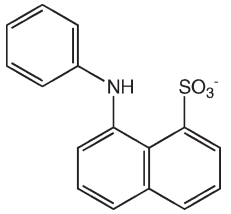

Figure 9. Structure of the 8-anilino-1-naphthalenesulfonic acid anion (ANS).

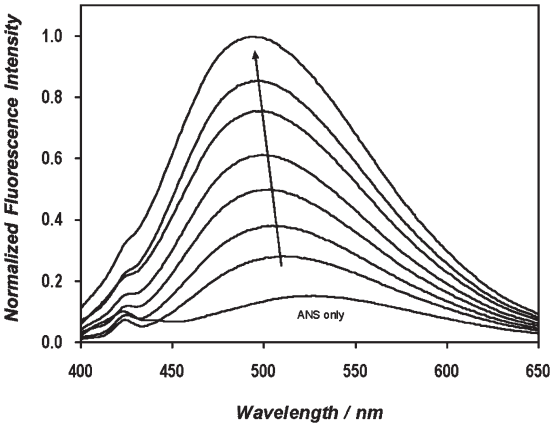

Figure 10. Fluorescence spectra of 20 μM ANS. Smallest intensity peak for no dendrimer added. Increasing intensities after addition of 59, 115, 198, 304, 500, 720, and 1255 μM G2.0 [50 mM NaCl, 5 mM Tris at pH 8.0, 23 °C, λ_{exc} = 370 nm].

PAMAM dendrimers and resulted in a binding constant between G5.0 PAMAM and ANS of about 1×10^5 M^{-1}.[52,53] The work described below extends ANS binding to PAMAM dendrimers to include the effect of dendrimer size and solution pH dependence upon binding constants.

Effects of PAMAM on ANS Emission. Adding PAMAM G2.0 (n = 16 amines) into a solution of buffered ANS causes an increase in the fluorescence intensity accompanied by a shift of the peak to shorter wavelengths (Figure 10). The increase in intensity means larger fractions of ANS molecules are binding to the added G2.0. Second, the blue shift from 526 to 496 nm by the end of the titration means the dendrimer microenvironment is less polar than water at pH 8. These changes are largest for the biggest dendrimers (Figure 11). If carried to completion, the shifts are quite dramatic, 54 nm for G4.0, 37 nm for G3.0, and 30 nm for G2.0, implying that this probe may be responding to very different microenvironments of dendrimers as a function of size in spite of the cationic charge of the dendrimer end groups at pH 8.

A 1:1 binding model is sufficient to describe the interaction between ANS and PAMAM dendrimers. Therefore, the fraction of bound ANS (X_b) is related to the free dendrimer concentration, [G_x], by a binding isotherm described shown in eq 14

$$X_b = \frac{K[G_x]}{1 + K[G_x]} \tag{14}$$

A complete derivation of the binding model using the fluorescence intensity data may be found in the Supporting Information. Figure 12 summarizes the fluorescence binding data along with the nonlinear fits to the binding equation for three different PAMAM dendrimers.

The binding constants extracted for ANS at pH 8 are 2200, 10 700, and 68 000 M^{-1} for G2.0, 3.0, and 4.0, respectively. Based on the fluorescence peak shifts and the previous work

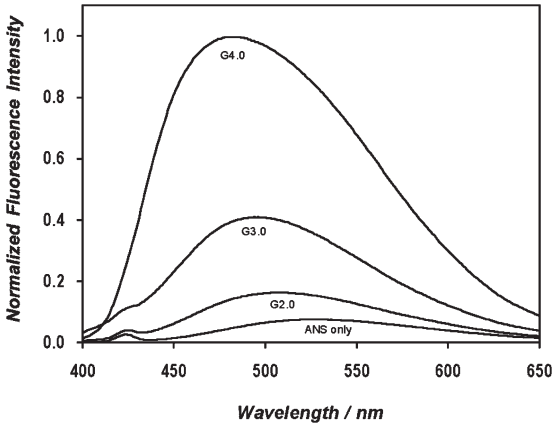

Figure 11. Fluorescence spectra for 20 μM ANS dissolved in 5 mM Tris, pH 8 (50 mM NaCl added). Bottom to top are for ANS only, added G2.0, G3.0, and G4.0 (85 μM each).

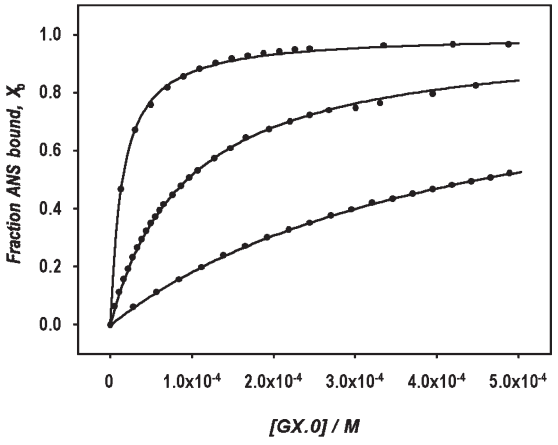

Figure 12. Plots for the fraction of bound ANS, X_b, versus free dendrimer concentration. Bottom to top: G2.0, G3.0, and G4.0. Curves are fits according to eq 14.

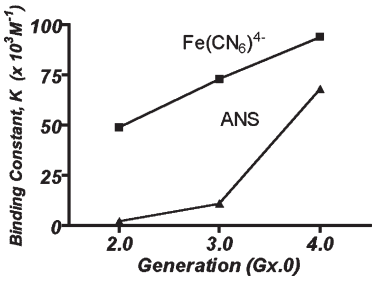

Figure 13. Comparison of PAMAM binding constants for ferrocyanide (upper data) and ANS (lower data). Conditions: 5 mM Tris pH 8.0 and 50 mM NaCl.

cited above, the ANS binding constants must be a combination of electrostatic and hydrophobic interactions with PAMAM dendrimers, while ferrocyanide binding should be entirely electrostatic. This becomes apparent when the binding constants are plotted together as a function of dendrimer size (Figure 13). Note that the *ratio* of ferrocyanide to ANS binding constants decreases (22:1, 7:1, and 1.4:1) from G2.0 to G4.0. This decreasing binding ratio and the increasing blue shift for the ANS probe with larger dendrimers are supporting evidence that the higher generation dendrimers are more hydrophobic due to their self-organization into more spherical molecules. It must be kept in mind that we use two different models for fitting the ferrocyanide data and the

ANS data. The main difference is that the ferrocyanide model uses a site binding assumption, while the ANS model assumes a molecular interaction (1:1 binding ratio).

Effect of pH on ANS−Dendrimer Binding. PAMAM dendrimers have sets of primary and tertiary amines that become protonated at different acidity levels.[28] From potentiometric titration curves in refs 27 and 28, one can estimate that the interior amines drop from about 15% protonated at pH 6 to 0% by pH 8, while the exterior primary amines are 100% protonated at pH 6 and drop to about 80−90% protonated by pH 8. While the conditions used in this study are not the same as those cited, one might predict that electrostatic binding of the ANS anion should be more important at pH 6 than 8. Chen et al. concluded that electrostatic binding of DNS (5-(dimethylamino)-1-naphthalenesulfonic acid) to G6 PAMAM was pH dependent and required conformational changes to account for the observed polarity changes (increased polarity as the pH dropped below 8.3).[54] Our results show that for G3.0 the ANS fluorescence *increases* upon raising the pH. The calculated binding constants change from 5400 to 7200 to 10 700 M^{-1} for pH 6 to 7 to 8 (data not shown). This effect of pH on binding is contrary to our hypothesis that electrostatics should be more important for PAMAM dendrimers at lower pH. We speculate that for the ANS probe the hydrophobic binding must outweigh the electrostatic component for ANS as pH is raised in this limited range or that hydrogen bonding between the dendrimer primary amines and the ANS secondary amine may play some role. In addition, we have ignored the possibility that ANS and ferrocyanide binding to PAMAM dendrimers somehow changes the local degree of protonation or of the hydrodynamic radius, as occurred for ANS binding to proteins cited above. It is perhaps more prudent to simply state that increasing the pH of the solution from 6 to 8 (which reduces the overall dendrimer polarity) enhances the binding of ANS to PAMAM dendrimers.

Conclusions

The methodology and binding isotherms needed to extract binding properties between small charged molecules and PAMAM dendrimers in buffered aqueous solutions are presented. The use of the electrostatic diffusional quenching method for $*Ru(bpy)_3^{2+}$ and the direct binding of ANS to dendrimers are fast, precise, and require very little material. Much of the work presented here builds on the work of others studying small molecule binding to macromolecules, yet the use of dendrimer macromolecules reveals differences in binding that one can control by selection of the appropriate soluble dendrimer (i.e., the size, the density, the charge/hydrophobicity of end groups, and, to some extent, the shape can be controlled). The ability to extract calculated values for small molecule binding constants, bound quenching rate constants, and especially the binding site size gives insight into the microenvironment of these dendrimers that has not been reported previously. It seems clear that the local microenvironment of these types of dendrimers can be understood and controlled. Therefore, future applications could benefit from a detailed knowledge of how the size and end groups of a given dendrimer platform, plus the solution composition, affect physical properties such as small molecule binding. We are actively pursuing such studies in aqueous solution and on dendrimer-modified surfaces.

Acknowledgment. This work was supported by the University of San Francisco Faculty Development Fund, The Lily Drake Fund, and a FIPSE grant for purchase of the fluorimeter.

Supporting Information Available: Derivation of the binding isotherm for ANS to dendrimers. This material is available free of charge via the Internet at http://pubs.acs.org.

References and Notes

(1) Tomalia, D. A.; Baker, H.; Dewald, J.; Hall, M.; Kallos, G.; Martin, S.; Roeck, J.; Ryder, J.; Smith, P. *Polym. J.* **1985**, *17*, 117–132.
(2) Newkome, G. R.; Yao, Z.; Baker, G. R.; Gupta, V. K. *J. Org. Chem.* **1985**, *50*, 2003–2004.
(3) Liang, C.; Frechet, J. M. J. *Prog. Polym. Sci.* **2005**, *30*, 385–402.
(4) Helms, B.; Liang, C. O.; Hawker, C. J.; Frechet, J. M. J. *Macromolecules* **2005**, *38*, 5411–5415.
(5) Baker, L. A.; Sun, L.; Crooks, R. M. *Bull. Korean Chem. Soc.* **2002**, *23*, 647–654.
(6) Kleij, A. W.; Ford, A.; Jastrzebski, J. T. B. H.; van Koten, G. *Dendritic Polymer Applications: Catalysts*; John Wiley & Sons Ltd.: West Sussex, 2001; Vol. Chapter III.6.
(7) McNerny, D. Q.; Kukowska-Latallo, J. F.; Mullen, D. G.; Wallace, J. M.; Desai, A. M.; Shukla, R.; Huang, B.; Banaszak Holl, M. M.; Baker, J. R. *Bioconjugate Chem.* **2009**, *20*, 1853–1859.
(8) Kim, Y.; Klutz, A. M.; Jacobson, K. A. *Bioconjugate Chem.* **2008**, *19*, 1660–1672.
(9) Cheng, Y.; Wu, Q.; Li, Y.; Xu, T. *J. Phys. Chem. B* **2008**, *112*, 8884–8890.
(10) Myc, A.; Majoros, I. J.; Thomas, T. P.; Baker, J. R. *Biomacromolecules* **2006**, *8*, 13–18.
(11) Majoros, I. J.; Myc, A.; Thomas, T.; Mehta, C. B.; Baker, J. R. *Biomacromolecules* **2006**, *7*, 572–579.
(12) Livramento, J. B.; Sour, A.; Borel, A.; Merbach, A. E.; Toth, E. *Chem.—Eur. J.* **2006**, *12*, 989–1003.
(13) Venditto, V. J.; Regino, C. A. S.; Brechbiel, M. W. *Mol. Pharmaceutics* **2005**, *2*, 302–311.
(14) Langereis, S.; deLussanet, Q. G.; vanGenderen, M. H. P.; Backes, W. H.; Meijer, E. W. *Macromolecules* **2004**, *37*, 3084–3091.
(15) Stiriba, S.-E.; Frey, H.; Haag, R. *Angew. Chem., Int. Ed.* **2002**, *41*, 1329–1334.
(16) Syahir, A.; Tomizaki, K.-y.; Kajikawa, K.; Mihara, H. *Langmuir* **2009**, *25*, 3667–3674.
(17) Longtin, R.; Maroni, P.; Borkovec, M. *Langmuir* **2009**, *25*, 2928–2934.
(18) Cahill, B. P.; Papastavrou, G.; Koper, G. J. M.; Borkovec, M. *Langmuir* **2008**, *24*, 465–473.
(19) Juttukonda, V.; Paddock, R. L.; Raymond, J. E.; Denomme, D.; Richardson, A. E.; Slusher, L. E.; Fahlman, B. D. *J. Am. Chem. Soc.* **2006**, *128*, 420–421.
(20) Knecht, M. R.; Sewell, S. L.; Wright, D. W. *Langmuir* **2005**, *21*, 2058–2061.
(21) Zhou, T.; Neubert, H.; Liu, D. Y.; Liu, Z. D.; Ma, Y. M.; Kong, X. L.; Luo, W.; Mark, S.; Hider, R. C. *J. Med. Chem.* **2006**, *49*, 4171–4182.
(22) Xu, Y.; Zhao, D. *Ind. Eng. Chem. Res.* **2006**, *45*, 7380–7387.
(23) Ye, H.; Crooks, R. M. *J. Am. Chem. Soc.* **2005**, *127*, 4930–4934.
(24) Xu, Y.; Zhao, D. *Environ. Sci. Technol.* **2005**, *39*, 2369–2375.
(25) Diallo, M. S.; Christie, S.; Swaminathan, P.; Johnson, J. H.; Goddard, W. A. *Environ. Sci. Technol.* **2005**, *39*, 1366–1377.
(26) Tomalia, D. A.; Naylor, A. M.; Goddard, W. A.III *Angew. Chem., Int. Ed.* **1990**, *29*, 138–175.
(27) Cakara, D.; Kleimann, J.; Borkovec, M. *Macromolecules* **2003**, *36*, 4201–4207.
(28) Niu, Y.; Sun, L.; Crooks, R. M. *Macromolecules* **2003**, *36*, 5725–5731.
(29) Moreno-Bondi, M. C.; Orellana, G.; Turro, N. J.; Tomalia, D. A. *Macromolecules* **1990**, *23*, 910–912.
(30) Turro, N. J.; Barton, J. K.; Tomalia, D. A. *Acc. Chem. Res.* **1991**, *24*, 332–340.
(31) Topp, A.; Bauer, B. J.; Klimash, J. W.; Spindler, R.; Tomalia, D. A.; Amis, E. J. *Macromolecules* **1999**, *32*, 7226–7231.
(32) Lyulin, A. V.; Davies, G. R.; Adolf, D. B. *Macromolecules* **2000**, *33*, 6899–6900.
(33) Kulczynska, A.; Frost, T.; Margerum, L. D. *Macromolecules* **2006**, *39*, 7372–7377.
(34) Kalsbeck, W. A.; Thorp, H. H. *J. Am. Chem. Soc.* **1993**, *115*, 7146–7151.
(35) Niu, S.; Turro, C.; Bossmann, S. H.; Tomalia, D. A.; Turro, N. J. *J. Phys. Chem.* **1995**, *99*, 5512–5517.

(36) Carter, M. T.; Rodriguez, M.; Bard, A. J. *J. Am. Chem. Soc.* **1989**, *111*, 8901–8911.
(37) Mansfield, M. L.; Klushin, L. I. *Macromolecules* **1993**, *26*, 4262–4268.
(38) Murat, M.; Grest, G. S. *Macromolecules* **1996**, *29*, 1278–1285.
(39) Harris, D. C. *Quantitative Chemical Analysis*, 6th ed.; W.H. Freeman: New York, 2003.
(40) Juris, A.; Manfrin, M. F.; Maestri, M.; Serpone, N. *Inorg. Chem.* **1978**, *17*, 2258–2261.
(41) Juris, A.; Gandolfi, M. T.; Manfrin, M. F.; Balzani, V. *J. Am. Chem. Soc.* **1976**, *98*, 1047–1048.
(42) Creutz, C.; Sutin, N. *J. Am. Chem. Soc.* **1976**, *98*, 6384–6385.
(43) Schwarz, P. F.; Turro, N. J.; Tomalia, D. A. *J. Photochem. Photobiol., A* **1998**, *112*, 47–52.
(44) Welch, T. W.; Thorp, H. H. *J. Phys. Chem.* **1996**, *100*, 13829–13836.
(45) Aslanoglu, M.; Isaac, C. J.; Houlton, A.; Horrocks, B. R. *Analyst* **2000**, *125* (10), 1791–1798.
(46) Zhang, Z.; Yu, X.; Fong, L. K.; Margerum, L. D. *Inorg. Chim. Acta* **2001**, *317*, 72–80.
(47) Gopidas, K. R.; Leheny, A. R.; Caminati, G.; Turro, N. J.; Tomalia, D. A. *J. Am. Chem. Soc.* **1991**, *113*, 7335–7342.
(48) *Handbook of Chemistry and Physics*, 75th ed.; CRC: Boca Raton, FL, 1995.
(49) Naylor, A. M.; Goddard, W. A.; Kiefer, G. E.; Tomalia, D. A. *J. Am. Chem. Soc.* **1989**, *111*, 2339–2341.
(50) Stryer, L. *Science* **1968**, *162*, 526–533.
(51) Matulis, D.; Baumann, C. G.; Bloomfield, V. A.; Lovrien, R. E. *Biopolymers* **1999**, *49*, 451–458.
(52) Shcharbin, D.; Klajnert, B.; Mazhul, V.; Bryszewska, M. *J. Fluoresc.* **2003**, *13*, 519–524.
(53) Shcharbin, D.; Szwedzka, M.; Bryszewska, M. *Bioorg. Chem.* **2007**, *35*, 170–174.
(54) Chen, W.; Tomalia, D. A.; Thomas, J. L. *Macromolecules* **2000**, *33*, 9169–9172.